ELSEVIER

Journal of Power Sources 92 (2001) 81–87

JOURNAL OF POWER SOURCES

www.elsevier.com/locate/jpowsour

Improved rapidly-quenched hydrogen-absorbing alloys for development of improved-capacity nickel metal hydride batteries

Tadashi Ise*, Takeo Hamamatsu, Teruhiko Imoto, Mitsuzo Nogami, Shinsuke Nakahori

Twicell Division, Soft Energy Company, Sanyo Electric Co. Ltd., 139-32 Toyohisa, Matsushige-cho, Itano-Gun, Tokushima 771-0213, Japan

Received 5 January 2000; received in revised form 18 May 2000; accepted 19 May 2000

Abstract

The effects of annealing a rapidly-quenched hydrogen-absorbing alloy with a stoichiometric ratio of 4.76 were investigated concerning its hydrogen-absorbing properties, crystal structure and electrochemical characteristics. Annealing at 1073 K homogenized the alloy microstructure and flattened its plateau slope in the P–C isotherms. However, annealing at 1273 K segregated a second phase rich in rare earth elements, increased the hydrogen-absorbing pressure and decreased the hydrogen-absorbing capacity. As the number of charge–discharge cycles increases, the particle size distribution of the rapidly-quenched alloy became broad due to partial pulverization. However, particle size distribution of the rapidly-quenched, annealed, alloy was sharp, since the annealing homogenized the microstructure, thereby improving the cycle characteristics.

A high-capacity rectangular nickel metal hydride battery using a rapidly-quenched, annealed, surface-treated alloy for the negative electrode and an active material coated with cobalt compound containing sodium for the positive electrode was developed. The capacity of the resulting battery was 30% greater than that of a conventional battery.

Keywords: Hydrogen-absorbing alloy; Nickel metal hydride battery; Rapidly quenching; Annealing

1. Introduction

The technology for secondary batteries has made rapid progress as the use and popularity of portable personal electronic devices such as cellular phones and laptop computers has increased rapidly. Because of the down-sizing of electronic devices and requirement for increased operating times, secondary batteries demand high-energy densities. Nickel metal hydride batteries are now seen as promising high-capacity portable power sources, owing to progress in the development of negative and positive electrodes.

Nickel metal hydride batteries consist of nickel hydroxide as the positive electrodes and hydrogen-absorbing alloys as the negative electrodes. The hydrogen-absorbing alloys can absorb 1000 times their own volume of hydrogen and have superior electrochemical reactivity. However, the capacity of the negative electrode need to be about 1.5 times larger than that of the positive electrode because the hydrogen-absorbing alloy used as the negative electrode are deteriorated during charge–discharge cycle. High corrosion resistance of hydrogen-absorbing alloys is an important subject.

Since the positive electrode determines the battery capacity, the high capacity of nickel metal hydride batteries is directly related to the high capacity of the positive electrodes. It has been reported that the use of nickel hydroxide modified by a cobalt compound containing sodium led to increased utilization of discharge electricity [1].

Since the negative electrodes do not determine the battery capacity directly, it is effective for the high capacity of nickel metal hydride battery by reducing the amount of negative electrode material and increasing that of positive electrode material instead. In this case, high corrosion-resistance and high discharge ability of the negative electrode materials are necessary in order to keep electrochemical characteristics, charge–discharge cycle life and high rate discharge ability, of the battery reducing the negative electrode material. The combination with high-capacity positive electrodes has also made it necessary to improve negative electrodes.

Hydrogen-absorbing alloy of AB_5 rare-earth-nickel-type have been used as negative electrode materials, owing to their high corrosion-resistance and high reactivity in alkali solutions. It has been reported that when rare-earth-nickel-type alloys were used as a base metal, partial replacement of cobalt with nickel improved corrosion resistance [2], while partial replacement of aluminum or manganese with nickel

* Corresponding author. Fax: +81-88-699-3991.
E-mail address: ise@sm.energy.sanyo.co.jp (T. Ise).

0378-7753/01/$ – see front matter
PII: S0378-7753(00)00501-2

[3] or an alloy with a stoichiometric ratio (the ratio of nickel to rare earth) under 5 increased hydrogen-absorbing capacity [4]. However, increased hydrogen-absorbing capacity also shortens the cycle life, because of greater alloy volume expansion and pulverization during charge–discharge cycles [5]. Therefore, it is important to realize higher hydrogen-absorbing capacity and minimizing pulverization.

For the purpose of achieving high corrosion-resistance, several preparation processes for hydrogen-absorbing alloys has been investigated [6]. Rapidly quenching homogenized the alloy composition at the microstructural level, and that annealing this alloy further reduced crystal lattice strain [7,8].

A charge transfer reaction is believed to occur at the interface between the electrolyte and the metal-rich (e.g. nickel) layer of an alloy surface [5]. In order to increase the number of charge–discharge reaction sites, surface treatment of a hydrogen absorbing alloy have also been investigated [9].

The technologies described above improve capacity, cycle life, and discharge ability. However, creating an effective battery requires an optimal combination of these techniques. This paper reports on the results of a study of the effects on the microstructure, hydrogen-absorbing properties, and pulverization behavior during cycles by annealing a rapidly-quenched alloy with a stoichiometric ratio of 4.76. The result led to the demand for improved battery cycle life. The study also demonstrated that surface treatment of the alloys improved discharge ability.

Using this modified alloy and a nickel hydroxide coated cobalt compound containing sodium, we developed a high capacity rectangular nickel metal hydride battery of the type used in cellular phones. The electrochemical properties of this battery were investigated.

2. Experimental details

2.1. Alloy preparation

An alloy with the composition $MmNi_{3.15}Co_{0.85}Al_{0.19}Mn_{0.57}$ [4,8], was prepared by induction melting; then solidified on a water-cooled roll, as a rapidly-quenched alloy. This sample was called sample A. Samples B and C were produced by annealing the alloy at 1073 and 1273 K, respectively, in an argon atmosphere. Sample D was prepared by a conventional production method, namely induction melting, and solidified in a water-cooled mold. The alloys (samples A, B, C, and D) were mechanically ground into powder of an average diameter of 50 μm.

Sample A, B, and C were analyzed by X-ray powder diffraction, using Cu Kα radiation, diffractometer and a monochromator of graphite, and scanning at speed of 1.0°/min and sampling pitch of 0.027°. It was reported to be appropriate to confirm the existence of a second phase [4] and the microstructure [7,8].

The pressure–composition isotherm properties of these alloys were measured by the Sieverts method at 313 K after three times repeatedly evacuating at 353 K and then loading with hydrogen at 298 K.

One sample of the annealed alloy at 1073 K was stirred in hydrochloric acid (pH 1) for 10 min and rinsed in water, producing sample E, a rapidly-quenched, annealed, and surface-treated alloy.

2.2. Measurement of cycle characteristics of hydrogen-absorbing alloys

In order to investigate the effects on the cycle characteristics caused by annealing of the rapidly-quenched alloy and its surface treatment, the hydrogen-absorbing-alloy electrode was prepared by mixing each of samples A, B, and E with polyetheleneoxide; then coating these slurries on punched metal collectors, and finally they were dried and rolled. These electrodes, which were used as negative electrodes, together with non-sintered nickel hydroxide electrodes were used to construct an experimental AA-size nickel metal hydride battery with a capacity of 1250 mA h. These batteries were charged at 250 mA for 16 h and discharged at 250 mA, until cell voltage fell to 1.0 V for two cycles. Charge–discharge cycle tests were then conducted at 1250 mA, with the $-\Delta V$ method and cut-off method used for the charging and discharging processes, respectively, in order to measure the change of battery capacity.

Alloy powder were removed from the batteries under charge–discharge cycles after the first, 50, 100, and 400 cycles. The particle size distribution of the removed alloy powders was then measured by laser diffraction. Mean diameters and relative standard deviations of particle sizes were calculated from the distributions and used as an index of particle distribution. Larger relative standard deviations indicated a broad distribution.

2.3. Measurement of electrochemical characteristics of hydrogen-absorbing alloys

In order to investigate the effects on the high-rate discharge characteristics caused by annealing of rapidly-quenched alloy and its surface treatment, test electrodes were prepared by mixing and then molding 0.5 g of each of the alloys A, B, and E with 0.4 g of carbonyl-nickel powder and 0.1 g of polytetrafluoroethylene. A counter electrode of sintered nickel hydroxide plate with excessive capacity, a reference electrode of a sintered nickel hydroxide plate having 50% charge, and an electrolyte of 30 wt.% KOH were placed in a sealed half-cell, as shown in Fig. 1. The internal pressure of the cell was set at 0.5 MPa, with nitrogen gas.

The test cell was first charged at 50 mA/g for 8 h; then discharged at 200 mA/g until the negative electrode potential was −1.0 V against the reference electrode. The discharge capacity at 200 mA/g was called C_1. The cell was

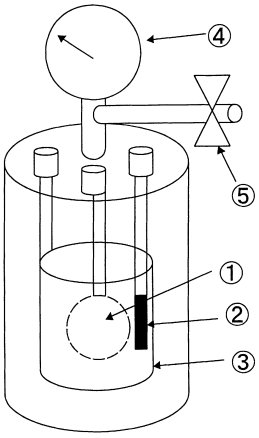

Fig. 1. Test cell for the electrochemical properties of hydrogen-absorbing alloy electrodes; (1) working electrode; (2) reference electrode; (3) counter electrode; (4) pressure gauge; (5) release valve.

discharged 60 min later at 50 mA/g until the negative electrode potential reached −1.0 V against the reference electrode. The discharge capacity at 50 mA/g was called C_2. An index of discharge ability was defined as $C_1/(C_1+C_2)$.

2.4. Preparation of nickel hydroxide coated with cobalt compound containing sodium

Nickel hydroxide powder, including cobalt and zinc [3], was placed into an aqueous solution of cobalt sulfate. The nickel hydroxide surface was coated with cobalt hydroxide by dropping sodium hydroxide solution. This coated nickel hydroxide powder was oxidized by atmospheric oxygen at 353 K under the coexistence of a sodium hydroxide solution, producing nickel hydroxide modified with a highly-conductive cobalt compound containing sodium.

The test electrode was prepared by filling this nickel hydroxide powder into a porous nickel substrate. A counter electrode of sintered cadmium plate having excessive capacity, a reference electrode of sintered cadmium plate, and an electrolyte of 30 wt.% KOH were placed in the same half-cell, as shown in Fig. 1. The cell was first charged at 30 mA/g for 16 h, and then discharged at 100 mA/g until the negative electrode potential was 1.0 V against the reference electrode. Capacity per gram of nickel hydroxide was measured.

2.5. Preparation of a nickel metal hydride battery, using modified positive and negative materials

A rectangular nickel metal hydroxide battery was designed and prepared with the dimensions 17.0 mm×48.0 mm×6.1 mm. A negative electrode consisting of a rapidly-quenched, annealed and surface-treated alloy, and a positive electrode of nickel hydroxide coated with a cobalt compound containing sodium were incorporated into the battery.

After activation, the battery was charged at 88 mA for 16 h and discharged at 176 mA until the cell voltage was 1.0 V. It was then compared with a previous battery type using an induction-melted alloy as the negative electrode and nickel hydroxide mixed with cobalt hydroxide powder as the positive electrode. The high-rate discharge characteristics of the batteries were then measured by charging at 88 mA for 16 h and discharging at 176, 440, 880, 1760 and 2640 mA. Charge–discharge cycle characteristics were measured by charging at 880 mA until $-\Delta V$ was 10 mV, and discharging at 880 mA until the cell voltage was 1.0 V.

3. Results and discussion

3.1. P–C isotherm properties of hydrogen-absorbing alloys

Fig. 2 shows the pressure–composition isotherm properties of these alloys. The plateau slope of the P–C isotherm diagram for the rapidly-quenched alloy, sample A, was much flatter than for the induction-melted alloy, sample D and was also observed to demonstrate a larger hydrogen-absorbing capacity at normal pressures. The plateau slope for the rapidly-quenched and annealed alloy, sample B, was flatter than for the other alloys. However, annealing the rapidly-quenched alloy at 1273 K led to increased equilibrium hydrogen pressure and reduced hydrogen-absorbing capacity.

It is well known that an induction-melted alloy has large segregation of manganese and the equilibrium hydrogen pressure varies locally [10]. This was believed to explain the higher value of the plateau slope. As contrasted with the induction-melted alloy (D), the composition of the rapidly-quenched alloy (A) was homogeneous, and the plateau of this alloy was flat. The flatter plateau slope has been explained to be due to annealing causing homogenous composition and removal of crystal lattice strain [7,8].

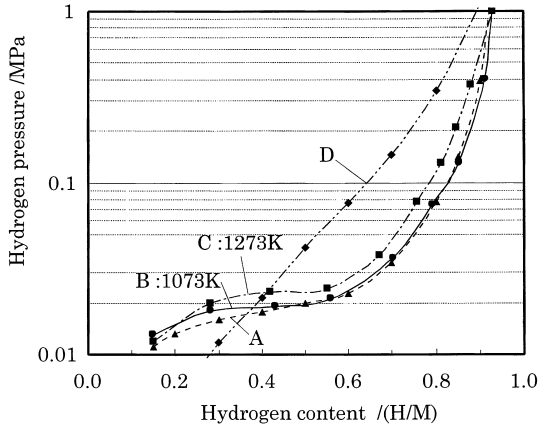

Fig. 2. P–C isotherms of the hydrogen absorbing alloys at 313 K: (◆) induction-melted; (▲) rapidly-quenched; (●) rapidly-quenched and annealed at 1073 K and (■) rapidly-quenched and annealed at 1273 K.

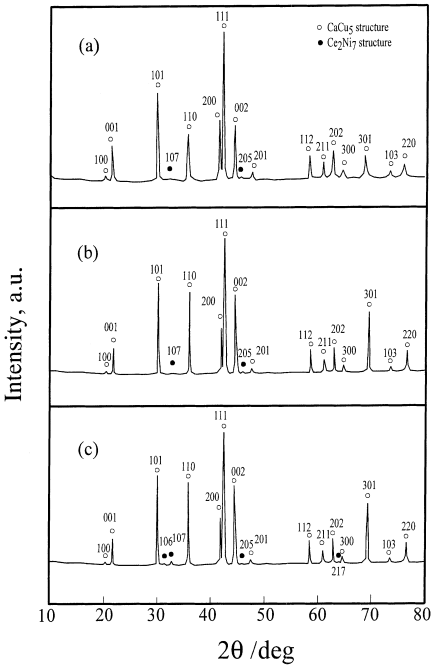

Fig. 3. X-ray diffraction patterns: (a) rapidly-quenched; (b) rapidly-quenched and annealed at 1073 K; (c) rapidly-quenched and annealed at 1273 K.

The factors increasing the equilibrium hydrogen pressure of the alloy annealed at 1273 K are discussed below in relation to X-ray diffraction patterns.

3.2. Microstructure

3.2.1. X-ray diffraction patterns

Fig. 3 provides X-ray diffraction patterns for the rapidly-quenched alloy (A) and the rapidly-quenched (B) and annealed alloys (C). Diffraction peaks from the $CaCu_5$ structure and several small peaks were observed in every sample. Nogami et al. investigated a microstructure of a rare-earth-nickel-type alloy with stoichiometric ratio of 4.17 by XRD, and observed several peaks from Ce_2Ni_7 [4]. Since our observed small peaks agreed with the peaks observed by Nogami et al., a second phase of an A_2B_7 phase having Ce_2Ni_7 structure was considered to exist.

The lattice parameters of the *a*- and *c*-axes were estimated by the least squares method against the *d*-values of the fifteen peaks identified as the $CaCu_5$-type structure. The standard deviation was calculated from deviations between estimated and measured *d*-values. An average value of full width and half-maximum (FWHM) calculated from four peaks at (1 0 0), (1 1 0), (1 1 1), and (2 0 0) was defined as an index of homogenization of an alloy. Table 1 provides unit cell volumes, lattice parameters and FWHMs. The unit cell volume of the alloy annealed at 1073 K was nearly equal to that of the alloy without annealing. However, for the alloy annealed at 1273 K, the unit cell volume (especially the lattice parameter of the *a*-axis) decreased. Moreover the FWHM of the annealed alloys decreased.

3.2.2. Discussion of microstructure

3.2.2.1. Homogenization of microstructure. It was found that annealing reduced FWHM and crystal lattice strain. This result agrees with the P–C isotherm properties, where annealing led to flattened plateau slopes.

3.2.2.2. Phase separation and composition change of the bulk phase. The separation of A_2B_7 was thought to progress by annealing at 1273 K because the small peaks in Fig. 3c are lager than in Fig. 3a and b. The stoichiometric ratio of the bulk is considered to increase by separating a second phase rich in rare-earth metal. It is known that an equilibrium hydrogen pressure increases as the stoichiometric ratio increase [4,6,11]. Increasing the equilibrium hydrogen pressure of the alloy annealed at 1273 K is considered to be due to increase in the stoichiometric ratio of the bulk.

3.2.2.3. Lattice parameters and unit cell volume. It is known that the unit cell volume of crystal lattices becomes smaller as stoichiometric ratios increase [4,6,11]. It was presumed that the reason for lower unit cell volumes after annealing at 1273 K was the increased stoichiometric ratio of the bulk phase. It was found that the primary change involved the lattice parameter of the *a*-axis. It is known that in the $LaNi_5$ system, the lattice parameter of the *a*-axis decreases, while that of the *c*-axis increases as stoichiometric ratios increase. However, it was thought that the effects for lattice parameter *c* would be small for alloys having stoichiometric ratios <5, since the cause of the expansion of lattice parameter *c* was assumed to be the substitute dumbbell-shaped nickel for lanthanum [6,11]. The substituted elements were also believed to affect the lattice parameter in multicomponent alloys [12]. Reduced unit cell volumes led to increased equilibrium pressures and decreased hydrogen-absorbing capacity [13].

Table 1
Crystallographic data for hydrogen-absorbing alloys

	Lattice constants		Unit cell volume (Å^3)	FWHM (°)
	a (Å)	*c* (Å)		
Rapidly quenched	4.999±0.004	4.057±0.004	87.80±0.14	0.323±0.005
Rapidly quenched and annealed at 1073 K	5.000±0.004	4.057±0.003	87.83±0.13	0.205±0.005
Rapidly quenched and annealed at 1273 K	4.994±0.003	4.056±0.003	87.60±0.11	0.149±0.005

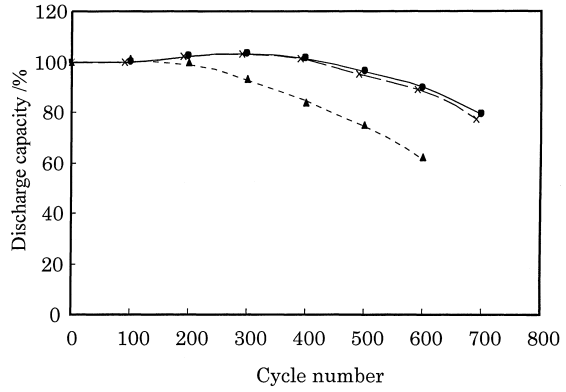

Fig. 4. Charge–discharge cycle characteristics: (▲) rapidly-quenched; (●) rapidly-quenched and annealed; (×) rapidly-quenched, annealed and surface-treated. Charge condition: current=1250 mA; △ V=−10 mV; discharge condition: current=1250 mA; cut-off voltage=1.0 V.

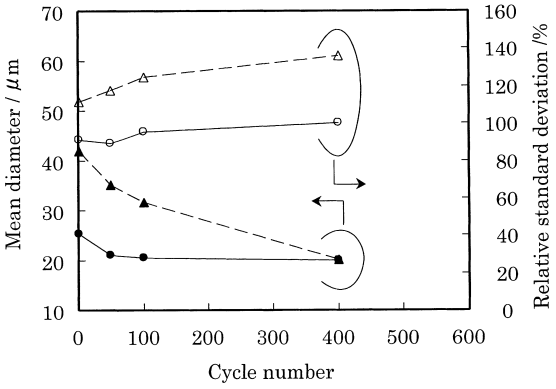

Fig. 6. Mean diameter (●▲) and relative standard deviation (○△) of hydrogen-absorbing alloy particles: (▲△) rapidly-quenched; (●○) rapidly-quenched and annealed.

3.3. Charge–discharge cycle characteristics of hydrogen-absorbing alloys

Fig. 4 shows the relationship between cycle number and discharge capacities for the rapidly-quenched alloy (A) and the rapidly-quenched and annealed alloy with/without surface treatment (B and E, respectively). Annealing of the rapidly-quenched alloys dramatically improved cycle characteristics. Surface treatment does not affect cycle characteristics.

Following the number of cycles, distribution of the particle sizes was studied. Fig. 5 shows the distribution of particle sizes after 2 and 100 cycles. The particle diameter was larger and the particle size distribution for the rapidly-quenched alloy (A) were broader than for the rapidly-quenched and annealed alloy (B). This tendency was remarkable for an alloy having sustained 100 cycles. The change of particle size distribution following the number of cycles is shown in Fig. 6 together with the relative standard deviations. The rapidly-quenched alloy has gradually been pulverized and the standard deviation has increased following the cycle number. On the other hand, it was found that the distribution of particle sizes for the rapidly-quenched and annealed alloy was almost invariable, and the standard deviations were small.

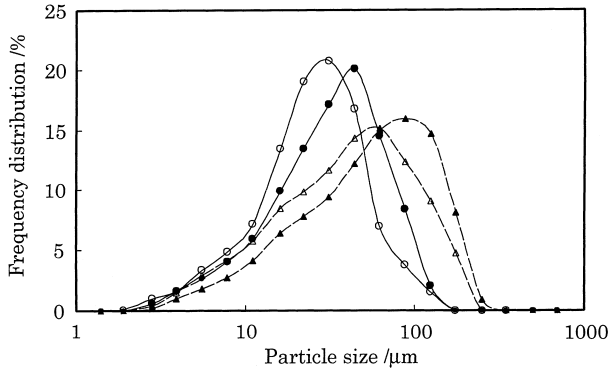

Fig. 5. Particle size distribution of hydrogen-absorbing alloys after two cycles (▲●) and after 100 cycles (△○): (▲△) rapidly-quenched; (●○) rapidly-quenched and annealed.

A discussion of several possible explanations follows. Nakamura et al. investigated rapid quenching alloys with/without annealing by SEM and EPMA, but could not confirm the change of the alloys with/without annealing [7]. It is considered that the distribution of elements between the alloy with/without annealing is not different. We considered the different pulverization behavior in view of cast structures. It is known that the cast structure of the part contacting with a mold become a chill structure and that of the other part become a columnar structure when molten metal cools in a mold [14]. Crystal grains of a chill structure are smaller than those of a columnar structure. Especially in the case of the rapidly quenched alloy, it was thought that pulverization was not homogeneous due to the differences in cast structure between the cooling side (a chill structure) and non-cooling side (a columnar structure) of the alloy. This could explain the broader particle size deviations following the number of cycles.

3.4. Discharge characteristics of hydrogen-absorbing alloys

Fig. 7 shows the discharge abilities $C_1/(C_1+C_2)$. The indices for the rapidly-quenched alloy (A) and rapidly-quenched and annealed alloy without surface treatment (B) were 77 and 75%, respectively. Annealing had little effect on these alloys. The index for rapidly-quenched, annealed, surface-treated alloy (E) was 89%, a remarkable increase in discharge ability.

It is known that rare-earth oxides and nickel metal forms on the alloy surface [15]. It has been reported that the porous metal layer of nickel or cobalt is formed by acid treatment as a result of efforts to solve the rare earth oxides. The porous surface may have increased the reaction surface area, while

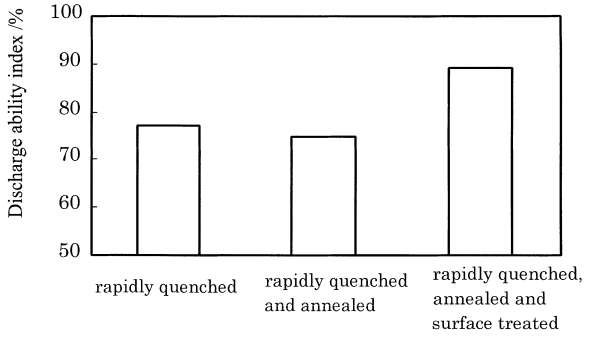

Fig. 7. Discharge ability index $C_1/(C_1+C_2)$ of the hydrogen-absorbing alloys.

the reactive sites on the formed metal layer improved discharge ability. These effects led to dramatic improvements in electrode activity.

3.5. Characteristics of the positive active material

The capacity of the nickel hydroxide modified by a conductive cobalt compound containing sodium was 332 mA h/g, 10% higher than for nickel hydroxide with cobalt oxide powder (303 mA h/g).

In order to analyze the factors which contribute to the effective utilization of active material, the quantity of sodium ions contained in the electrode before and after discharge was measured by an atomic absorption method. The results showed that the sorption–desorption amount of sodium in the nickel hydroxide modified by a cobalt compound was larger than that of unmodified nickel hydroxide. It is known that the sorption–desorption amount of sodium increases as the reaction electron number of nickel hydroxide increases [3]. We found that coating nickel hydroxide with the sodium containing cobalt compound increases conductivity on the particle surface and charge acceptance.

3.6. Characteristics of nickel metal hydride battery using modified positive and negative active materials

Fig. 8 shows the discharge curve of the rectangular nickel metal hydride battery using the nickel hydroxide modified by a cobalt compound containing sodium for the positive electrode, and a rapidly-quenched, annealed, surfaced-treated alloy for the negative electrode (E). The capacity of the modified battery was approximately 900 mA h, almost 30% higher than that of a previous battery (700 mA h).

Fig. 9 gives high-rate discharge characteristics, showing that capacity exceeded 700 mA h, while voltage exceeded 1.1 V at 2640 mA. The modified battery exhibited superior discharge characteristics.

Fig. 10 shows charge–discharge cycle characteristics. When the charge–discharge cycles were repeated at 880 mA, the discharge capacity of the modified battery

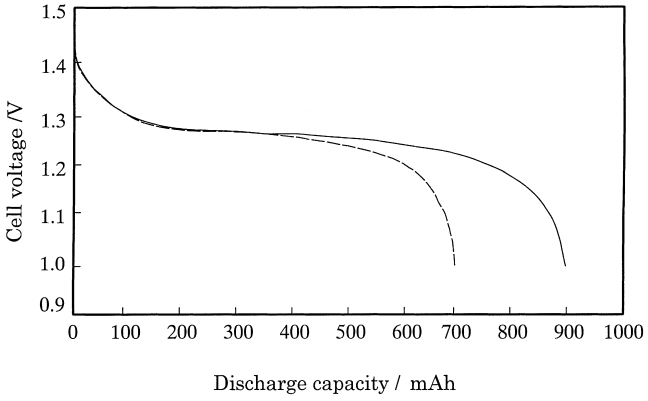

Fig. 8. Effect of the new active materials on discharge characteristics: (- - -) a conventional cell; (——) a cell using the new active materials. Charge condition: current=88 mA for 16 h; discharge condition: current=176 mA; cut-off voltage=1.0 V.

was about 90% at 500 cycles, comparing favorably to the conventional battery.

In summary, new design of technologies to get high performances of positive and negative materials can play significant roles in the development of battery technology.

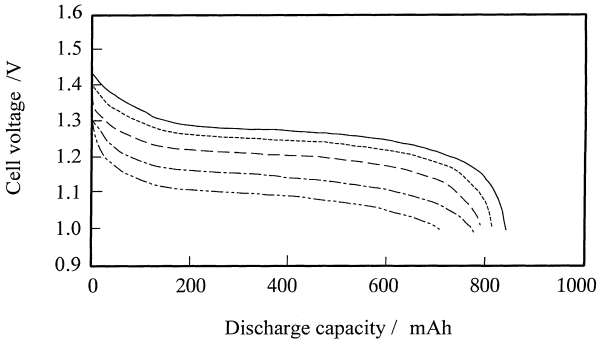

Fig. 9. Discharge characteristics of a cell using the new active materials. Charge condition: current=88 mA for 16 h; discharge condition: current=176 mA (——), 440 mA (- - -), 880 mA (– – –), 1760 mA (– · – · – ·), 2640 mA (– ·· – ·· – ·); cut-off voltage=1.0 V.

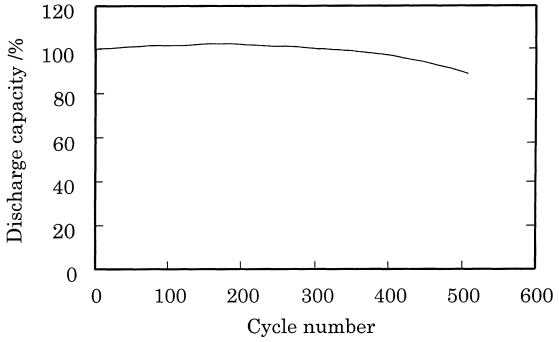

Fig. 10. Charge–discharge cycle characteristics of a cell using the new active materials. Charge condition: current=880 mA; ΔV=−10 mV; discharge condition: current=880 mA, cut-off voltage=1.0 V.

4. Conclusions

Annealing and surface treatment with an acid solution were used to modify a rapidly-quenched alloy with a stoichiometric ratio of 4.76 to get high capacity and structural homogeneity. The following three conclusions could be made:

1. Annealing of a rapidly-quenched alloy homogenized crystal structure, cast structure, and pulverization behavior, and also improved cycle life.
2. Annealing at elevated temperature (1273 K) caused the separation of a second phase from the bulk phase, and reduced hydrogen-absorbing capacity. The optimal annealing temperature was found to be 1073 K.
3. Acid-solution surface treatment of rapidly-quenched and annealed alloys improved high-rate discharge characteristics, but had no effect on cycle characteristics.

We have thus developed a rectangular nickel metal hydride battery incorporating the modified alloy and a nickel hydroxide modified with a cobalt compound containing sodium. The resulting battery has 30% higher capacity than an earlier battery, superior high-rate discharge characteristics, and long cycle life. Use of such batteries can extend operating life for popular portable electronic devices such as cellular phones.

References

[1] M. Yano, K. Shinyama, M. Nogami, S. Nakahori, M. Tadokoro, I. Yonezu, K. Nishio, Abstracts of the Electrochemical Society of Japan, 17–18 September 1996, p. 4.
[2] T. Sakai, K. Oguro, H. Miyamura, N. Kuriyama, A. Kato, H. lshikawa, J. Less-Common Metals 161 (1990) 193.
[3] M. Nogami, N. Furukawa, J. Chem Soc. Jpn. 1 (1995) 1.
[4] M. Nogami, M. Tadokoro, M. Kimoto, Y. Chikano, T. Ise, N. Furukawa, Denki Kagaku 61 (1993) 1088.
[5] J.J.G. Willems, K.H. Buschow, J. Less-Common Metals 129 (1987) 13.
[6] P.H.L. Notten, J.L.C. Daams, R.E.F. Einerhand, Ber. Bunsenges. Phys. Chem. 96 (1992) 656.
[7] Y. Nakamura, H. Nakamura, S. Fujitani, I. Yonezu, J. Alloys Comp. 210 (1994) 299.
[8] T. Imoto, M. Kimoto, N. Higashiyama, S. Fujitani, K. Nishio, Denki Kagaku 66 (1998) 1088.
[9] T. Imoto, K. Kato, N. Higashiyama, M. Kimoto, Y. Itoh, K. Nishio, J. Alloys Comp. 282 (1999) 274.
[10] S. Fujitani, S. Yasuyama, A. Furukawa, T. Yonesaki, K. Nasako, I. Yonezu, T. Saito, J. Japan Inst. Metals 56 (1992) 965.
[11] K.H.J. Bushow, H.H. Vanmal, J. Less-Common Metals 29 (1972) 203.
[12] Y. Osumi, H. Suzuki, A. Kato, K. Oguro, S. Kawai, M. Kaneko, J. Less-Common Metals 74 (1980) 271.
[13] H.H. Mendelsohn, D.M. Gruen, A.E. Dwight, J. Less-Common Metals 63 (1979) 193.
[14] G.J. Davies, Solidification and Casting, Elsevier, England, 1990.
[15] W.E. Wallace, H. Imamura, J. Phys. Chem. 83 (1979) 1708.